J. Geophys. 42, 407–417, 1977

Journal of Geophysics

Original Investigations

Structure of Lunar Impact Craters from Gravity Models

P. Janle

Institut für Geophysik der Universität, Bundesstr. 55/XIV, D-2000 Hamburg 13, Federal Republic of Germany

Abstract. Bouguer anomalies for the lunar impact craters Copernicus, Theophilus, and Ptolemaeus have been computed. Copernicus and Theophilus have Bouguer gravity minima. Gravity models assume a zone of ruptured rocks below the craters.

Ptolemaeus has a strong Bouguer maximum. An isostatic upwelling of the mantle and instrusions of mantle material have been assumed in the gravity model. Ptolemaeus may be regarded as an intermediate structure between isostatically undercompensated craters and mascon-maria.

Key words: Lunar impact craters – Bouguer gravity – Gravity models.

1. Introduction

Many meteoric impact craters are known on the Earth. Their main structural properties are a basin, a ring wall, and a zone of breccia and ruptured rocks below the crater floors (Fig. 1a). This ruptured zone causes the negative Bouguer gravity of most of the terrestrial impact craters (Innes, 1961; Angenheister and Pohl, 1969; Jung et al., 1969). Low altitude Doppler gravity data with a resolution of 20–50 km, which permit model calculations, exist for only a few lunar impact craters. Sjogren et al. (1974c) modelled the negative gravity anomaly of the crater Copernicus. They replaced the topographic mass deficit and the rim by surface disks. However, they needed for their model a density of 3.57 g/cm^3 which is far too high in contrast to 2.6 g/cm^3 of the uppermost crust. In order to reduce the density value, the authors suggested a less dense debris layer below the crater.

Many of the maria represent another type of characteristic impact structures on the Moon (Fig. 1c). The formation of these structures can be described as follows: High-energetic large meteorites had excavated large, mostly circular basins. The resulting mass deficiency was partly compensated by an isostatic or dynamic upwelling of the mantle. Intrusions of mantle material penetrated

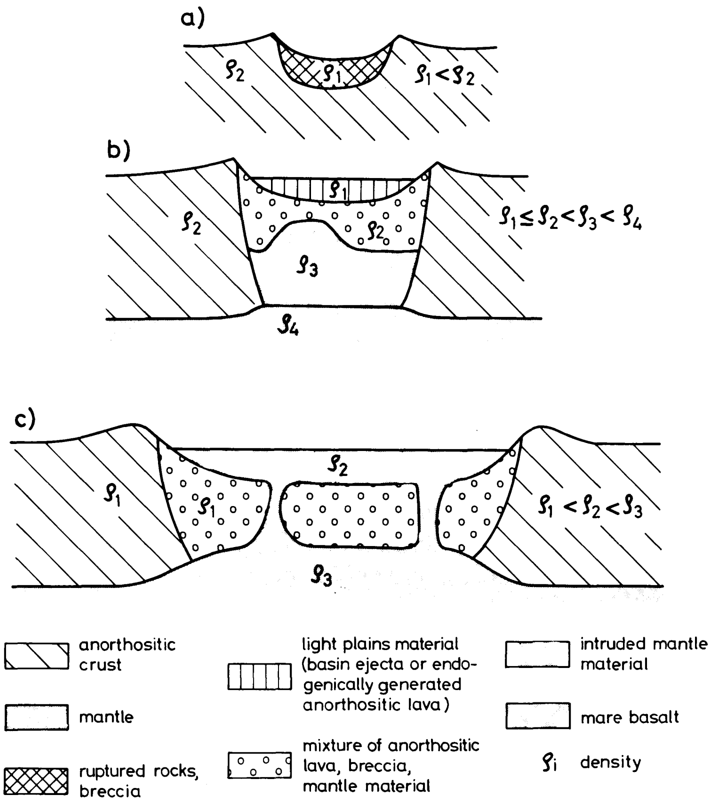

Fig. 1a–c. Lunar impact structures. **a** isostatically undercompensated crater, **b** endogenically modified crater or basin, **c** mascon-mare (isostatically overcompensated model)

the thinned, fractured crust and filled the basins to overcompensation with basaltic lavas. The mass surplusses, which cause the enormous free air gravity anomalies of some 100 mgal, are called "mascons" (Wise and Yates, 1970; Phillips et al., 1974). Kunze (1974) suggested a model in which the mass surplusses are compensated isostatically by mass deficits at depth. The mascon possessing maria are also called "mascon-maria".

So far only free air gravity models have been calculated without accurately considering the topographic effects. In this paper, Bouguer anomalies for the craters Copernicus, Theophilus, and Ptolemaeus will be presented and models of the depth structures will be computed (Fig. 2).

2. Calculation of the Bouguer Anomalies

The gravity data used in this paper are from Kunze (1975). Kunze converted the line-of-sight accelerations to vertical gravity values which were normalized

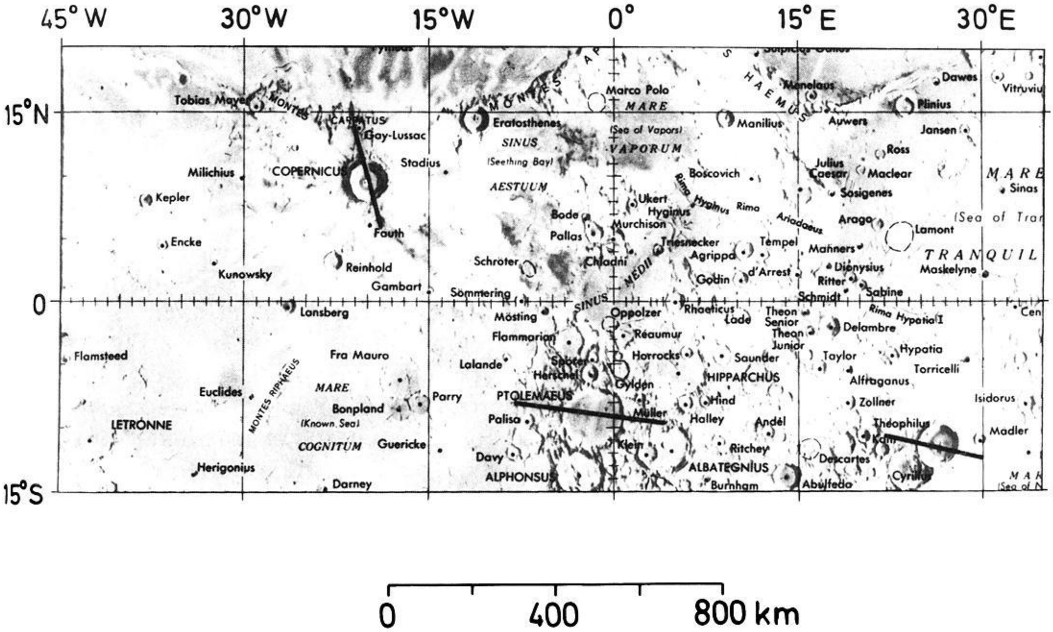

Fig. 2. Profile location

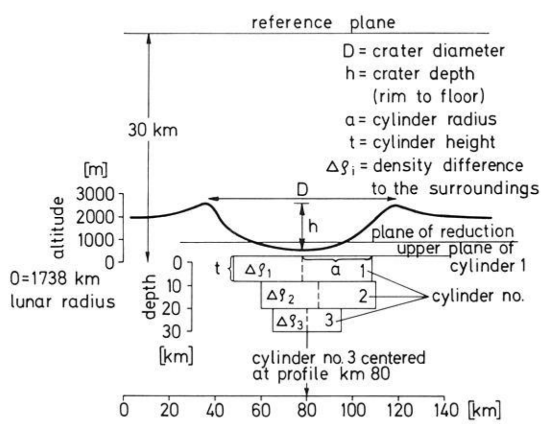

Fig. 3. Schematic crater model illustrating the elements for the calculation of the Bouguer anomalies and the gravity models

to 30 km altitude above mean lunar radius. Only the data of the southern part of Copernicus are unconverted; they correspond to a flight height of about 30 km according to Sjogren et al. (1974a). Nevertheless, the effects of amplitude decrease and angular shift for these data are small because Copernicus lies near the subearth point. The gravity values were enhanced by 30% in order to compensate for the effect of the least squares filter of the orbit determination program. This program derives the Doppler residuals from the tracking data (Gottlieb, 1970; Sjogren et al., 1972).

The Doppler gravity can be interpreted as free air gravity referred to a reference plane of 30 km altitude in this case.

Figure 3 shows the elements for the calculation of the Bouguer gravity and the gravity models. All altidude and depth values in the figures and in the text are referred to a normal datum of 1738 km mean lunar radius. The altitude data of the profiles and for the terrain correction are from Lunar Aeronautic Charts (LAC, 1962). The terrain correction removes the gravity effects of topographic masses above and below the plane of reduction which is the mean level of the crater floor. It was calculated up to a distance of 100 km using the formula for a cylindrical slice with a Bouguer density of 2.6 g/cm^3.

Kunze (1975) does not discuss the accuracy of his gravity maps. But errors of 10 mgal seem to be reasonable. A density variation of 0.1 g/cm^3 causes a variation of 6 mgal for a terrain correction of 150 mgal. An accuracy of 100 m for relative heights is given on the LAC charts. A maximum error of 300 m is assumed for height determinations of the terrain correction causing an error of 10 mgal. The resulting mean error is ± 15 mgal for the Bouguer gravity.

Figures 4–6 present the free air gravity, terrain correction, and Bouguer gravity for the three craters investigated.

3. Model Calculations

Copernicus (Fig. 4) and Theophilus (Fig. 5) have Bouguer gravity minima. Therefore the free air minima cannot be modelled simply by replacing the topographic mass deficit and the rim by surface disks as it was done in previous works (Sjogren et al., 1974c). As mentioned in the introduction the deficit density for these previous models is far too high. This suggests to compare the depth structures of lunar impact craters with their terrestrial analogues.

Many terrestrial impact craters have Bouguer minima which are caused by ruptured zones below the craters (Innes, 1961). Considering the stress tensor, the following formula can be derived for the depth parameter of the ruptured zone (Beals et al., 1963):

$$R = \sqrt[4]{S_{\text{shear}}/(8\, S_{\text{comp}})}\; D$$

D = crater diameter,
R = depth of the reptured zone relative to the undisturbed topography,
S_{shear} = tensile strength to cause rupture,
S_{comp} = compressive strength to cause rupture.

For granitic gneiss Beals et al. calculated $R = 1/3\ D$ with $S_{\text{comp}} = 1.6 \times 10^3$ and $S_{\text{shear}} = 0.16 \times 10^3$ kg/cm^2. Jaeger (1969) gives for gabbro $S_{\text{comp}} = 1.8 \times 10^3$ kg/cm^2; Chung (1972) found that the elastic properties of lunar samples are about the same as those of similar terrestrial rocks. Considering that lunar anorthosite

Table 1. Crater and model parameters (compare with Fig. 3), all lengths in km, $\Delta\rho$ in g/cm³

	Diameter D	Depth h	Altitude of the plane of reduction	Model peak anomalies (mgal)
Copernicus	93	3.3	−0.1	− 30
Theophilus	100	4.4	1.9	−116
Ptolemaeus	153	1.0–1.5	1.1	+ 92

	Altitude of upper plane	Radius a	Height t	Centered at prof. km	$\Delta\rho$	Radius a	Height t	Centered at prof. km	$\Delta\rho$	Radius a	Height t	Centered at prof. km	$\Delta\rho$
	cylinder 1					cylinder 2				cylinder 3			
Copernicus	−0.1	36	10	138	−0.15	32	10	138	−0.1	25	9	138	−0.1
Theophilus	1.9	30	25	150	−0.45	25	15	150	−0.4				
Ptolemaeus	30	75	15	200	0.05	70	16	200	0.1	80	4	195	0.3
	cylinder 4					cylinder 5				cylinder 6			
Ptolemaeus	0	30	30	255	0.2	30	15	250	0.15	50	16	220	0.1

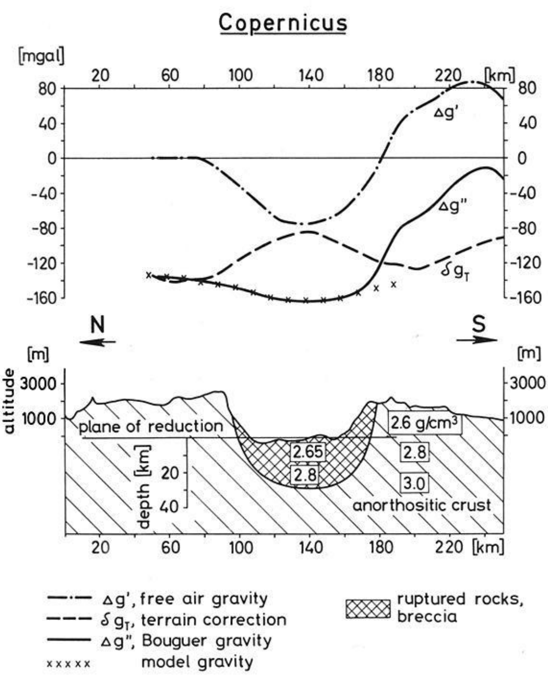

Fig. 4. Copernicus. Reference plane for the gravity anomalies at 30 km altitude; plane of reduction for the terrain correction at −0.1 km altitude

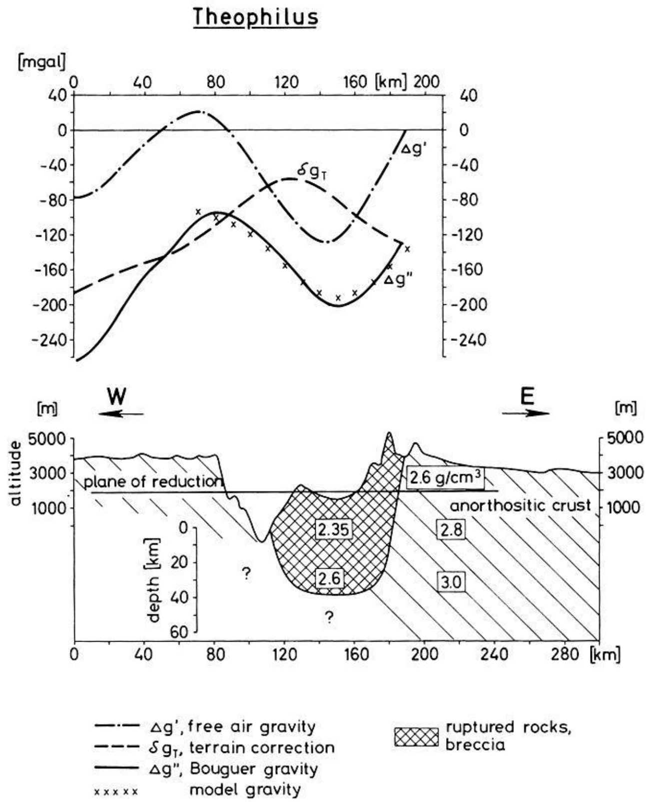

Fig. 5. Theophilus. Reference plane for the gravity anomalies at 30 km altitude; plane of reduction for the terrain correction at 1.9 km altitude

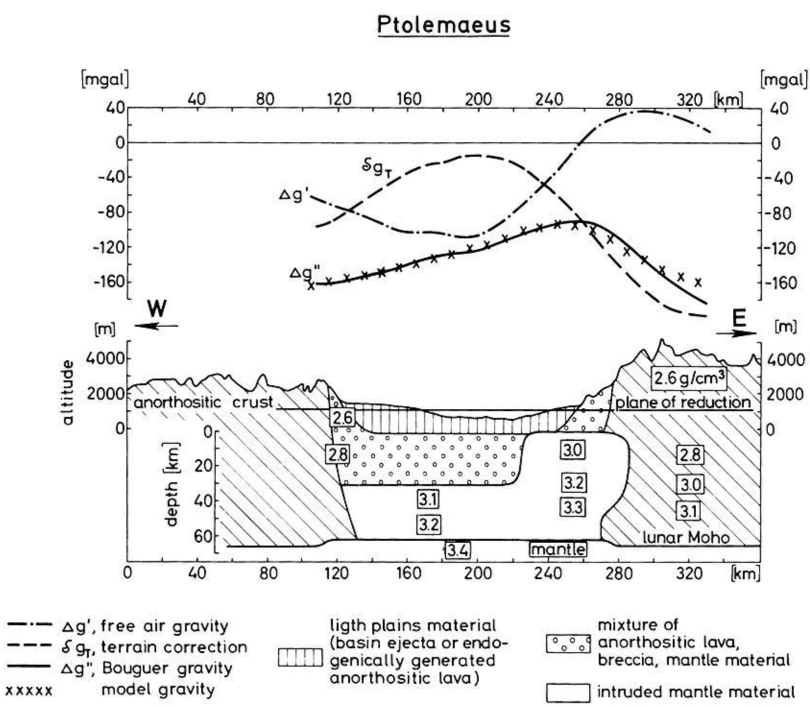

Fig. 6. Ptolemaeus. Reference plane for the gravity anomalies at 30 km altitude; plane of reduction for the terrain correction at 1.1 km altitude

comes petrologically close to gabbro and assuming a 50% variation of the ratio S_{shear}/S_{comp} – that means a variation of the factor 0.33 from 0.28 to 0.37 – the formula $R = 1/3\ D$ can be used as a first approximation also for lunar impact craters.

Another parameter for the model calculation is the density difference between the ruptured zone and the surrounding crust. For terrestrial craters it ranges between -0.1 g/cm^3 (e.g. Meteor Crater, Arizona (Regan and Hinze, 1975)) and -0.4 g/cm^3 (e.g. Deep Bay Crater, Canada (Innes, 1961)). For the lunar models the density difference was assumed to decrease slightly with increasing depth (see Copernicus and Theophilus, Table 1).

The form of the depth structure of the craters was modelled by several cylindrical disks (Fig. 3). Formulas for the gravity attraction of cylinders are from Telford et al. (1976). The crater and model parameters for the three craters investigated are summarized in Table 1.

The crater models of Figures 4–6 show absolute density values which are based upon publications of Solomon (1974) and Copper et al. (1974).

4. Description of the Craters

The three craters investigated are situated in transition zones between highlands and maria. The regional Bouguer anomalies are strongly negative. There is a general trend towards more negative values with increasing terrain elevations (Copernicus: -40 mgal↔2000 m; Theophilus: -200 mgal↔4000 m; Ptolemaeus: -160 mgal↔2500 m and -180 mgal↔4000 m; the plane of reduction for these examples is at 1.1 km altitude which is also the plane of reduction of Ptolemaeus).

These values indicate in general an isostatic behaviour of the lunar crust outside the craters.

Copernicus (Fig. 4) has a Bouguer gravity minimum and a model gravity of -30 mgal. The ruptured zone of the model reaches a depth of 29 km which is in agreement with the 1/3 relation. A moderate density difference of -0.15 g/cm^3 is assumed for the first cylinder and -0.1 g/cm^3 for the next two cylinders. No attempt has been made to model the gravity high south of Copernicus because there is no correlation between this high and the topography.

Theophilus (Fig. 5) shows a strong Bouguer minimum shifted 20 km to the east of the crater center. The pronounced free air and Bouguer gravity low west of the crater cannot be correlated with topographic features. The map of Kunze (1975) shows a local extent of this free air low. In this case it is diffecult to estimate the local anomaly for the model fit. The proposed model has a deficit density of -0.45 g/cm^3 for the first and -0.4 g/cm^3 for the second cylinder. These density differences are at the upper limit of corresponding terrestrial impact structures. The depth of the ruptured rocks should be 33 km according to the 1/3 relation; however, the model thickness of this zone is 43 km.

Local melting and intrusions of heavy mantle material in the western part of the crater could explain the shift of the gravity minimum. Possibly these intrusions also cause the local relative high gravity values in the region of the western rim.

These considerations would reduce the high negative crater anomaly and the associated high deficit density and great depth of the ruptured zone for the model gravity data to the east and to the south of the crater.

Ptolemaeus (Fig. 6) shows a strong Bouguer maximum shifted to the east of the crater. The model gravity amounts to 92 mgal. This result is in contradiction to model computations of Sjogren et al. (1974b). They explained the free air gravity low of Ptolemaeus by means of a topographic mass deficit and in addition to this a low density crater filling material; but they did not compute the gravity effect of the irregular topography in this region. According to Sjogren et al. (1972), Sjogren and Wollenhaupt (1973), and Sjogren et al. (1974b) the Apollo laser altimetry yields the effective crater depth of Ptolemaeus to be 500 m less than LAC chart 77 (effective depth is measured from the undisturbed topography to the crater floor). Recalculations of the terrain corrections for this higher crater floor show no qualitative change of the relative Bouguer high.

Following considerations have been made for the model computations.

The 1/3 relation yields a depth of 51 km for the ruptured zone. Pike (1967) derived a depth (h)/diameter (D) relation for large highland craters (Fig. 3):

$$h = 0.880\ D^{0.35}.$$

The resulting original depth of Ptolemaeus after the impact should be 5.1 km.

The topographic mass deficit and the ruptured crust caused an isostatic upwelling of the mantle which reduced the original crater depth. Considering an original crater depth of 5.1 km a density of 2.6 g/cm^3 for the uppermost crust, and a density difference of 0.3 g/cm^3 between the mantle and the lower crust, an upwelling of 4.5 km of the mantle is necessary for isostatic compensation. A 4 km upwelling has been assumed in the model calculations (cylinder 3 in Table 1) which, however, causes only about 1/8 of the Bouguer maximum. Intrusions of heavy mantle material have therefore been assumed to fit the rest of the maximum (cylinders 1, 2, 4, 5, 6 in Table 1). In the eastern part of the crater these intrusions come close to the surface. The rest of the original ruptured zone was less intruded by mantle material. This process equalized the density contrast to the surroundings. This model is consistent with the reduced present crater depth of about 1–1.5 km.

Other large craters like Humboldt and Posidonius have rilles on their crater floors which indicate an isostatic uplift and/or endogenic intrusional activity (Baldwin, 1971; Brennan, 1975). Such rilles are not visible on the crater floor of Ptolemaeus. They may either not exist or be covered by the crater filling classified as Cayley material. This material belongs to the light plains which can be found in more or less large patches over the entire surface of the Moon.

The discussion of the origin of the Cayley formation is controversial. Two possibilities have been proposed:

1. It is composed of basin ejecta from Imbrium or Orientale (Eggleton and Schaber, 1972; Chao et al., 1975).

2. It has been formed by other, perhaps endogenic, processes (Soderblom and Boyce, 1972; Neukum et al., 1975).

Chao et al. (1975) conclude a highly feldspathic composition of the Cayley material from investigations of samples. Geochemical remote sensing measurements (Adler et al., 1973) show no significant change in the chemical composition between the crater filling of Ptolemaeus and the neighbouring highland areas. These results exclude a high density crater filling by mantle or mare material. This statement favours the ejecta hypothesis.

Chao et al. (1975) assume a 2–3 km thick filling of Ptolemaeus with ejecta from the Orientale basin excavation. The density of this material may be equal or less than the surrounding density. A 2 km thick layer with a deficit density of -0.1 g/cm^3 contributes only -5 mgal to the gravity. Thus gravity calculations do not exclude a disk of basin ejecta.

According to relative age determinations of Soderblom and Boyce (1972), the Cayley formation cannot be part of basin ejecta blankets. Neukum et al. (1975) show that the cumulative crater frequency of the crater floor of Ptolemaeus lies between the Orientale and Imbrium frequency curves. These results favour an endogenic origin of some light plains.

Regarding the crater history of Ptolemaeus as proposed in this paper, one may assume that the intruded mantle material partly melted the original ruptured anorthositic zone. Some parts of the anorthositic lavas ascended to the crater floor forming a 2 km thick layer with no density contrast to the surrounding anorthositic crust. Therefore an endogenic origin of the crater filling is not in contradiction to the model proposed here.

The Vredefort Ring in South Africa may be a terrestrial analogue to Ptolemaeus. Its diameter of 100 km requires a ruptured zone of 33 km depth which is about crustal thickness. Dietz (1963) suggested an isostatic upwelling of the mantle for this structure which is in agreement with a positive residual gravity of 20–30 mgal (Uys and Enslin, 1970).

5. Conclusions

The Bouguer anomalies of the 3 investigated craters show that the neglect of the detailed topographic gravity effects leads to wrong interpretations of local free air gravity anomalies.

Copernicus and Theophilus have Bouguer gravity minima caused by a zone of ruptured rocks and breccia similar to terrestrial impact structures. No isostatic compensation of the mass deficit occurred. Both craters are of the type shown in Figure 1 a.

Ptolemaeus has a strong Bouguer maximum. Isostatic uplift of the mantle associated with endogenic intrusional activity of mantle material has been assumed for model calculations and crater history. A near surface mascon as found in mascon-maria has not been considered because there are no indications for near surface mantle or mare materials. Neither an ejecta origin nor an endogenous origin of the crater filling Cayley material can be excluded.

The proposed model shows that this large crater is an intermediate structure between isostatically undercompensated craters and mascon-maria. This type of craters may be termed "endogenically modified craters or basins". Figure 1b shows the structural properties of this type.

Acknowledgement. I thank Dr. A. Behle for reading the manuscript and helpful discussions.

References

Adler, I., Trombka, J.I., Lowman, P., Schmadebeck, R., Blodget, H., Eller, E., Yin, L., Lamothe, R., Osswald, G., Gerard, J., Gorenstein, P., Bjorkholm, P., Gursky, H., Harris, B., Arnold, J., Metzger, A., Reedy, R.: Apollo 15 and 16 Results of the integrated geochemical experiment. The Moon **7**, 487–504, 1973

Angenheister, G., Pohl, J.: Die seismischen Messungen im Ries von 1948–1969. In: Das Ries. Geologica Bavarica Nr. 61, E. Preuss, H. Schmidt-Kaler, ed., pp. 304–326. München: Straub 1969

Baldwin, R.G.: The question of isostasy on the Moon. Phys. Earth Planet. Interiors **4**, 167–179, 1971

Beals, C.S., Innes, M.J.S., Rottenberg, I.A.: Fossil Meteorite Craters. In: The moon, meteorites, and comets. B.M. Middlehurst, G.P. Kuiper, ed., pp. 235–284. Chicago: The University of Chicago Press 1963

Brennan, W.J.: Modification of premare impact craters by volcanism and tectonism. The Moon **12**, 449–461, 1975

Chao, E.C.T., Hodges, C.A., Boyce, I.M., Soderblom, L.A.: Origin of lunar light plains. J. Res. U.S. Geol. Survey **3**, 4, 379–392, 1975

Chung, D.H.: Laboratory studies on seismic and electrical properties of the moon. The Moon **4**, 356–372, 1972

Cooper, M.R., Kovach, R.L., Watkins, J.S.: Lunar near-surface structure. Rev. Geophys. and Space Phys. **12**, 291–308, 1974

Dietz, R.S.: Astroblemes: Ancient Meteorite-Impact Structures on the Earth. In: The Moon, Meteorites and Comets. B.M. Middlehurst, G.P. Kuiper, ed., pp. 285–300. Chicago: The University of Chicago Press 1963

Eggleton, R.E., Schaber, G.G.: Cayley formation interpreted as basin ejecta. In: Apollo 16, Prel. Sci. Rep. NASA SP-315, 29-7–29-16, 1972

Gottlieb, P.: Estimation of local lunar gravity features. Radio Sci. **5**, 301–312, 1970

Innes, M.J.S.: The use of gravity methods to study the underground structure and impact energy of meteorite craters. J. Geophys. Res. **66**, 2225–2239, 1961

Jaeger, J.C.: Elasticity, fracture and flow with engineering and geological applications, 3rd ed. London: Methuen 1969

Jung, K., Schaaf, H., Kahle, H.G.: Ergebnisse gravimetrischer Messungen im Ries. In: Das Ries. Geologica Bavarica Nr. 61, E. Preuss, H. Schmidt-Kaler, ed., pp. 337–342. München: Straub 1969

Kunze, A.W.G.: Lunar mascons: Another model and its implications. The Moon **11**, 9–17, 1974

Kunze, A.W.G.: Lunar Crustal Density Profile from an analysis of doppler gravity data. The Moon **12**, 101–112, 1975

LAC: Lunar Aeronautic charts LAC 1 through LAC 144, aeronautical chart and information center, 127 charts published, 1st ed. St. Louis, Mo.: 1962

Neukum, G., König, B., Fechtig, H., Storzer, D.: Cratering in the earth-moon system: Consequences for age determination by crater counting. In: Proc. Lunar Sci. Conf. 6th, 2597–2620, 1975

Phillips, R.I., Conel, J.E., Sjogren, W.L.: The nature of the circular maria based on gravity studies. Space Res. **14**, 635–645, 1974

Pike, R.J.: Schroeter's rule and the modification of lunar impact morphology. J. Geophys. Res. **72**, 2099–2106, 1976

Regan, R.D., Hinze, W.J.: Gravity and magnetic investigations of meteor crater, Arizona. J. Geophys. Res. **80**, 776–788, 1975

Sjogren, W.L., Gottlieb, P., Muller, P.M., Wollenhaupt, W.R.: Lunar gravity via Apollo 14 Doppler radio tracking. Science **175**, 165–168, 1972

Sjogren, W.L., Wollenhaupt, W.R.: Lunar shape via the Apollo laser altimeter. Science **179**, 275–278 1973

Sjogren, W.L., Wimberly, R.N., Wollenhaupt, W.R.: Lunar gravity via the Apollo 15 and 16 subsatellites. The Moon **9**, 115–128, 1974a

Sjogren, W.L., Wimberly, R.N., Wollenhaupt, W.R.: Lunar gravity: Apollo 16. The Moon **11**, 35–40, 1974b

Sjogren, W.L., Wimberly, R.N., Wollenhaupt, W.R.: Lunar gravity: Apollo 17. The Moon **11**, 41–52, 1974c

Soderblom, L.A., Boyce, J.M.: Relative ages of some near-side and far-side terra plains based on Apollo 16 metric photography. In: Apollo 16, Prel. Sci. Report, NASA SP-315, 29-3–29-6, 1972

Solomon, S.C.: Density within the moon and implications for lunar composition. The Moon **9**, 147–166, 1974

Telford, W.M., Geldart, L.P., Sheriff, R.E., Keys. P.A.: Applied geophysics. Cambridge-London-New York-Melbourne: Cambridge University Press 1976

Uys, N.J., Enslin, J.F.: Geological Map of the Republic of South Africa and the Kingdoms of Lesotho and Swaziland, 1:1000000. Gravity Edition. Department of Mines, Geological Survey 1970

Wise, D.U., Yates, M.T.: Mascons as structural relief on a lunar 'Moho'. J. Geophys. Res. **75**, 261–268, 1970

Received July 28, 1976; Revised Version November 19, 1976